The Canadian Mineralogist
Vol. 53, pp. 235-248 (2015)
DOI: 10.3749/canmin.1500005

BUSSYITE-(Y), A NEW BERYLLIUM SILICATE MINERAL SPECIES FROM MONT SAINT-HILAIRE, QUEBEC

JOEL D. GRICE, RALPH ROWE, AND GLENN POIRIER

Research Division, Canadian Museum of Nature, P.O. Box 3443, Station D, Ottawa, Ontario K1P 6P4

ABSTRACT

Bussyite-(Y), ideally $(Y,\mathit{REE},Ca)_3(Na,Ca)_6MnSi_9Be_5(O,OH,F)_{34}$, a new mineral species, was found in the Mont Saint-Hilaire quarry, Quebec, Canada. The crystals are transparent to translucent, dark brown, with a white streak and vitreous luster. Crystals are blocky to prismatic, sometimes radiating, up to 3 mm in size. The mineral is brittle with a perfect $\{\bar{1}01\}$ cleavage. Associated minerals include aegirine, analcime, calcite, cappelenite-(Y), catapleiite, charmarite-2*H* and -3*T*, fluorite, helvine, kupletskite, microcline, perraultite, sérandite, and tainiolite. Bussyite-(Y) is monoclinic, space group *C*2, with unit-cell parameters refined from X-ray powder-diffraction data: *a* 11.545(2), *b* 13.840(2), *c* 16.504(4) Å, β 95.87(2)º, *V* 2623.1(6) Å^3, and *Z* = 4. Electron microprobe analysis gave the average composition and ranges, in wt.%: Na_2O 8.21 (8.43–8.07), K_2O 0.08 (0.10–0.05), BeO 9.75 (determined by structure refinement), CaO 5.25 (5.36–5.16), MnO 2.93 (3.20–2.57), BaO 0.03 (0.06–0.00), FeO 0.40 (0.60–0.25), Al_2O_3 0.29 (0.34–0.21), Y_2O_3 7.58 (7.79–7.37), La_2O_3 0.48 (0.60–0.40), Ce_2O_3 2.66 (3.09–2.37), Pr_2O_3 0.55 (0.64–0.40), Nd_2O_3 2.85 (2.93–2.81), Sm_2O_3 1.45 (1.58–1.23), Eu_2O_3 0.013 (0.17–0.12), Gd_2O_3 1.97 (2.21–1.57), Tb_2O_3 0.31 (0.40–0.25), Dy_2O_3 2.20 (2.46–1.81), Ho_2O_3 0.39 (0.48–0.33), Er_2O_3 0.93 (1.07–0.86), Tm_2O_3 0.16 (0.20–0.12), Yb_2O_3 0.46 (0.60–0.36), Lu_2O_3 0.01 (0.01–0.01), Nb_2O_5 0.20 (0.25–0.15), SiO_2 39.62 (40.03–38.96), ThO_2 2.21 (2.43–1.90), F 3.49 (3.66–3.39), Cl 0.03 (0.03–0.02), H_2O 5.10 (determined by crystal-structure refinement), O = F + Cl – 1.48, total 98.15. The empirical formula based on the crystal-structure analysis showing 34 anions is: $4\{(Y_{0.874}Nd_{0.221}Ce_{0.211}Dy_{0.154}Gd_{0.142}Sm_{0.108}Er_{0.063}Pr_{0.043}La_{0.038}Yb_{0.030}Ho_{0.027}Tb_{0.022}Tm_{0.011}Eu_{0.010}Ca_{0.789}Th_{0.105})_{\Sigma 1}[Na_{3.442}Ca_{0.800}K_{0.022}]_{\Sigma 6.055}(Mn_{0.537}Fe_{0.072})_{\Sigma 0.899}(Si_{8.567}Be_{5.065}\ Al_{0.222})_{\Sigma 13.724}(O_{24.107}OH_{5.893})_{\Sigma 30}(F_{2.386}OH_{1.60.3}Cl_{0.011})_{\Sigma 4}\}$. The structure was refined to an R_1 index of 0.035 for 6531 unique, observed reflections. The structure has two chemically distinct layers parallel to $(\bar{2}01)$: (1) a layer of $[(Si,Be)O_4]$ tetrahedra and (2) a large cation Y-,Ca-, Mn-, Na-(O,F) polyhedral layer. Layers are cross-linked through shared O and F atoms. Significant amounts of OH are present, as indicated in the IR spectrum and crystal-structure analysis.

Keywords: bussyite-(Y), new mineral species, crystal structure, non-centrosymmetric, rare-earth elements, beryllium, infrared spectroscopy, hydrogen, Mont Saint-Hilaire, Quebec.

INTRODUCTION

The name, bussyite, honours the French chemist Antoine Alexandre Brutus Bussy (1794–1882). Bussy's main interest was pharmaceuticals, but he researched the preparation of magnesium and he and Friedrich Wöhler are each credited with independently isolating the element beryllium in August 1828 (Bussy 1828). The new mineral, a beryllium-silicate, is one of several beryllium-silicates found in alkaline intrusions. Alkaline intrusions were not included to any extent in the seminal work on the mineralogy, petrology, and geochemistry of beryllium (Grew 2002), but this occurrence is the main topic in the recent work of Raade (2008). Alkaline rocks are not an economic source of beryllium, but the element is essential in 37 mineral species occurring in syenitic pegmatites (Raade 2008). Of these, Raade (2008) lists 16 occurring at Mont Saint-Hilaire. An additional three minerals, beryl, beryllonite, and bussyite-(Ce), also occur there; all are listed below. Some of the minerals described are zeolites and warrant research into their sieving and exchange properties (Grice 2010).

The new mineral and its name have been approved by the Commission on New Minerals, Names and Classification (CNMNC), IMA (IMA #2014–060). The holotype specimen (catalogue #CMNMC 86870) is housed in the collection of the Canadian Museum of Nature, Ottawa, Ontario, Canada.

OCCURRENCE

Bussyite-(Ce) was found in a small alkaline pegmatite located in the main Poudrette quarry (level 7), Mont Saint-Hilaire, La Vallée-du-Richelieu RCM, Montérégie, Quebec, Canada. It occurs as embedded prismatic crystals inside massive white analcime. It is

differentiated from associated aegirine prisms by its rectangular cross section in broken crystals. Other associated minerals are: calcite, cappelenite-(Y), catapleiite, charmarite-2*H* and -3*T*, fluorite, helvine, kupletskite, microcline, perraultite, sérandite, and tainiolite. To date, 20 Be-bearing mineral species have been found at Mont Saint-Hilaire: barylite, bavenite, behoite, beryl, beryllonite, bussyite-(Ce), bussyite-(Y), chkalovite, eirikite, epididymite, eudidymite, genthelvite, helvine, hingganite-(Ce), hingganite-(Y), leifite, leucophanite, milarite, niveolanite, and tugtupite. Most of these species occur within or closely associated with a pegmatite.

Physical and Optical Properties

Bussyite-(Y) belongs to the monoclinic crystal system in the sphenoidal class, 2, whereas bussyite-(Ce) belongs to the prismatic class, 2/*m*. Crystals are blocky, prismatic to bladed, sometimes radiating, and measure up to 3 mm. Bussyite-(Y) is transparent to translucent, dark brown, with a white streak and vitreous luster. There is no fluorescence in either short-wave or long-wave ultraviolet light. It has an approximate hardness of 4 (Mohs hardness scale), is brittle and splintery, and has a perfect {101} cleavage. The density was not measured due to the small grain size; the calculated density is 3.11 g/cm^3.

Bussyite-(Y) is biaxial negative, α 1.583 ± 0.002, β 1.593 ± 0.002, γ 1.600 ± 0.002, $2V_{meas.}$ = 68(2)º, $2V_{calc}$ = 79º. Dispersion could not be observed, and there is no pleochroism. The optical orientation is: $Z \wedge \mathbf{c}$ = 33º (β obtuse), Y = **b**, and X = [101]. Fine lamellar twinning, parallel to the elongation, was seen in some crystals.

TABLE 1. CHEMICAL COMPOSITION FOR BUSSYITE-(Y) (*n* = 3)

Oxide	Oxide wt.%	Max	Min	Std. Dev.	Element	No. atoms
Na_2O	8.21	8.43	8.07	0.19	Na^+	3.449
K_2O	0.08	0.10	0.05	0.03	K^+	0.022
(BeO)	(9.75)				(Be^{2+})	(5.075)*
CaO	5.25	5.36	5.16	0.1	Ca^{2+}	1.219
FeO	0.40	3.20	2.57	0.32	Fe^{2+}	0.072
BaO	0.03	0.06	0	0.03	Ba^{2+}	0.003
MnO	2.93	0.60	0.25	0.18	Mn^{2+}	0.538
Al_2O_3	0.29	0.34	0.21	0.07	Al^{3+}	0.074
Y_2O_3	7.58	7.79	7.37	0.21	Y^{3+}	0.874
La_2O_3	0.48	0.60	0.40	0.10	La^{3+}	0.038
Ce_2O_3	2.66	3.09	2.37	0.38	Ce^{3+}	0.211
Pr_2O_3	0.55	0.64	0.40	0.14	Pr^{3+}	0.043
Nd_2O_3	2.85	2.93	2.81	0.07	Nd^{3+}	0.221
Sm_2O_3	1.45	1.58	1.23	0.19	Sm^{3+}	0.108
Eu_2O_3	0.13	0.17	0.12	0.03	Eu^{3+}	0.010
Gd_2O_3	1.97	2.21	1.57	0.35	Gd^{3+}	0.142
Tb_2O_3	0.31	0.40	0.25	0.08	Tb^{3+}	0.022
Dy_2O_3	2.20	2.46	1.81	0.35	Dy^{3+}	0.154
Ho_2O_3	0.39	0.48	0.33	0.08	Ho^{3+}	0.027
Er_2O_3	0.93	1.07	0.86	0.12	Er^{3+}	0.063
Tm_2O_3	0.16	0.20	0.12	0.04	Tm^{3+}	0.011
Yb_2O_3	0.46	0.60	0.36	0.12	Yb^{3+}	0.030
Lu_2O_3	0.01	0.01	0.01	0.00	Lu^{3+}	0.001
SiO_2	39.62	40.03	38.96	0.58	Si^{4+}	8.585
ThO_2	2.12	2.43	1.90	0.28	Th^{4+}	0.105
Nb_2O_5	0.20	0.25	0.15	0.05	Nb^{5+}	0.020
F	3.49	3.66	3.39	0.15	F^-	2.392
Cl	0.03	0.03	0.02	0.01	Cl^-	0.011
(H_2O)	(5.10)				(H^+)	(7.371)*
O = F	–1.47	–1.40	–1.54	–0.06	O^{2-}	31.597
O = CL	–0.01	0.00	–0.01	–0.01	———	
					CATSUM	21.116
TOTAL	98.15				AN SUM	34

*Based on crystal structure determination

Chemical Composition

Electron-microprobe analysis

Microanalysis (Table 1) was carried out using a JEOL 8230 electron microprobe at the University of Ottawa. The accelerating voltage was 20 kV with a 20 nA beam current and a 10 μm spot size. At these conditions, count rates were constant over the duration of the analyses (20 s peak, 10 s background). The following standards were used: REE*L*α, $REEPO_4$ (Cherniak *et al.* 2004); Na*K*α, albite; Fe*K*α, almandine; Ca*K*α, Mg*K*α, and Si*K*α, diopside; F*K*α, fluorite; Mn*K*α, Nb*L*α, columbite-(Mn); Ti*K*α, rutile; Ba*L*α, sanbornite; K*K*α, Al*K*α, sanidine; Th*M*α, ThO_2; Cl*K*α, tugtupite; Y*L*α, yttrium iron garnet; Zr*L*α, zircon. Raw counting data was corrected for overlap using empirical correction factors, and matrix corrections were done using a PAP correction (Pouchou & Pichoir 1984). Three full analyses were done.

The empirical formula, based on the crystal-structure analysis ideally showing 34 anions, is: $(Y_{0.874}Nd_{0.221}Dy_{0.154}Gd_{0.142}Sm_{0.108}Er_{0.063}Pr_{0.043}La_{0.038}Yb_{0.030}Ho_{0.027}Tb_{0.022}Tm_{0.011}Eu_{0.010}Th_{0.105}Nb_{0.020})_{\Sigma 1.868}$ $(Ca_{0.789}Ce_{0.211})_{\Sigma 1}$ $(Na_{3.449}Ca_{0.430}K_{0.022}Ba_{0.003})_{\Sigma 3.904}$ $(O_{24.107}OH_{5.893})_{\Sigma 30}$ $(Mn_{0.538}Fe_{0.072})_{\Sigma 0.610}$ $(Si_{8.585}Be_{5.075}Al_{0.074})_{\Sigma 13.73}$ $(F_{2.386}OH_{1.603}Cl_{0.011})_{\Sigma 4}$.

Infrared analysis

The infrared spectrum (Fig. 1) of bussyite-(Y) was obtained using a Bomen Michelson MB-120 Fourier-transform infrared spectrometer with a diamond-anvil cell microsampling device. The frequencies are not well resolved. There is a low, broad peak in the high-frequency range, 3500–2500 cm^{-1}, due to $[OH]^-$ stretching. There are four minor peaks in the 2500–2000 range due to $[OH]^-$ stretching. Comparing the remaining part of the spectrum to spectra given in Farmer (1974), the following frequency regions are assigned modes: the large, broad peak centered at 967 cm^{-1} is the $[SiO_4]$ and $[BeO_4]$ stretching mode with shoulders at 1008 and 1036 cm^{-1} likely due to the shorter bonds between Be and Si and OH and F; and the moderate intensity, sharper peaks centered at 859, 705, and 647 cm^{-1} are the $[SiO_4]$ and $[BeO_4]$ bending modes.

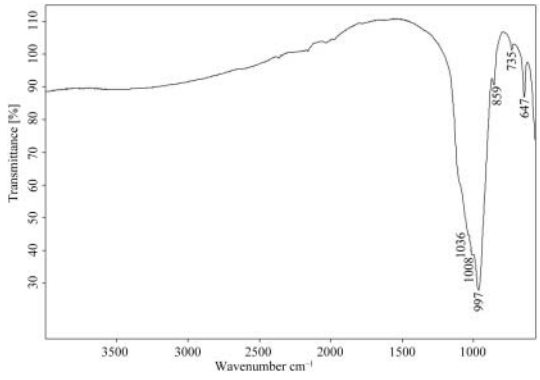

FIG. 1. The infrared spectrum for bussyite-(Y).

X-Ray Crystallography and Crystal-Structure Determination

X-ray diffraction data (Table 2) were acquired using a Bruker D8-Discover instrument equipped with a Hi-Star 2D detector and running GADDS Software calibrated with a statistical approach by Rowe (2009). A copper X-ray source was used for a $K\bar{\alpha}$ = 1.5418 Å. Unit-cell parameters refined from powder data are: *a* 11.545(2), *b* 13.840(2), *c* 16.504(4), β 95.87(2) Å, *V* 2623.1(6) $Å^3$, *Z* = 4. The bussyite-(Y) diffraction pattern exhibits a definite shift toward slightly larger *d*-spacings compared to bussyite-(Ce). This observation triggered a more thorough characterization of the specimen, leading to the discovery of the new species once the chemical composition was known.

To obtain a single crystal of bussyite-(Y), a fragment was trimmed to 10 × 30 × 70 μm. Intensity data were collected using a fully automated Bruker *P*4 four-circle diffractometer operated at 50 kV, 24 mA, with graphite-monochromated Mo*K*α radiation and a 4K APEX CCD detector at a 5 cm distance from the crystal. Integrated intensities were collected up to 2θ = 60º, using 16 s frame counts and a frame width of 0.3º. The unit-cell parameters for the single crystal were refined using 18223 indexed reflections. Data pertinent to the intensity-data collection are given in Table 3.

Reduction of the intensity data, structure determination, and structure refinement were done with the SHELXTL (Sheldrick 1990) package of computer programs. Data reduction included corrections for background, scaling, and Lorentz-polarization factors. An empirical absorption correction (SADABS, Sheldrick 1998) was applied. The merging $R_{(int)}$ for the complete dataset (39280 reflections) decreased from 0.084 before the absorption correction to 0.048 after the absorption correction. Merging symmetry-related reflections gave the following $R_{(int)}$ values; for *C* 2/*c*, 0.023 (3882 unique reflections), and for *C* 2, 0.020, (7762 unique reflections).

The starting parameters for the structure refinement were those determined for bussyite-(Ce) (Grice *et al.* 2009). The centrosymmetric structure in space group *C* 2/*c* (No. 15) refined to *R* = 0.043 and 0.038 (all data and observed data) but there were a large number of systematic absence exceptions for the *c*-glide, 1137 with 79 intensities greater than 3 sigma.

TABLE 2. X-RAY POWDER-DIFFRACTION DATA FOR BUSSYITE-(Y) Cu($K\alpha$)

I obs.	*I* calc. *	*d* obs.	*d* calc. **	hkl
7	4	8.830	8.838	1 1 0
100	**100**	**8.049**	**8.051**	**$\bar{1}$ 1 1**
9	5	7.539	7.538	1 1 1
21	**18**	**6.924**	**6.920**	**0 2 0**
5	3	6.263	6.265	$\bar{1}$ 1 2
6	6	5.273	5.291	0 2 2
9	6	4.482	4.497	1 1 3
	3		4.494	2 0 2
7	8	4.419	4.419	2 2 0
15	15	4.186	4.181	$\bar{1}$ 3 1
5	3	4.121	4.104	0 0 4
6	7	4.021	4.025	$\bar{2}$ 2 2
5	6	3.772	3.769	2 2 2
	4		3.689	3 1 0
	18		3.530	0 2 4
38	**21**	**3.529**	**3.526**	**3 1 1**
	2		3.497	$\bar{3}$ 1 2
21	**21**	**3.435**	**3.436**	**$\bar{1}$ 3 3**
	4		3.311	1 3 3
10	13	3.215	3.209	$\bar{3}$ 1 3
23	**18**	**3.155**	**3.160**	**$\bar{1}$ 1 5**
	8		3.133	$\bar{2}$ 2 4
	5		3.002	1 1 5
	4		2.964	2 4 0
35	**26**	**2.940**	**2.940**	**$\bar{3}$ 3 1**
	8		2.928	3 1 3
	3		2.924	0 4 3
	7		2.896	2 2 4
	3		2.871	4 0 0
50	**31**	**2.840**	**2.861**	**3 3 1**
	42		2.836	$\bar{2}$ 4 2
30	**23**	**2.736**	**2.736**	**0 0 6**
	3		2.684	$\bar{3}$ 3 3
	6		2.666	$\bar{1}$ 5 1
38	**19**	**2.651**	**2.655**	**$\bar{1}$ 3 5**
	6		2.652	4 2 0
	7		2.645	0 4 4
	2		2.645	1 5 1
30	**17**	**2.629**	**2.628**	**4 0 2**
	4		2.559	1 3 5
6	5	2.472	2.474	$\bar{4}$ 0 4
	2		2.465	$\bar{2}$ 4 4
	2		2.413	$\bar{2}$ 2 6
	3		2.377	2 0 6
15	15	2.343	2.345	2 4 4
	3		2.341	3 1 5
	3		2.312	$\bar{1}$ 1 7
	3		2.309	$\bar{3}$ 1 6
14	4	2.305	2.307	0 6 0
	8		2.303	4 2 3
8	7	2.274	2.276	$\bar{1}$ 5 4
10	9	2.246	2.243	3 5 0
14	7	2.218	2.221	0 2 7
	3		2.209	4 4 0
	2		2.165	$\bar{4}$ 2 5
	3		2.146	0 4 6
	3		2.121	$\bar{3}$ 5 3
4	3	2.091	2.093	4 4 2
	3		2.091	$\bar{2}$ 6 2
7	8	2.064	2.064	$\bar{5}$ 3 1
	3		2.057	1 5 5
	2		2.033	3 5 3
8	9	2.013	2.013	$\bar{4}$ 4 4
4	4	1.9979	1.9983	$\bar{2}$ 0 8
	3		1.9388	$\bar{1}$ 7 1
	2		1.9309	1 7 1
	6		1.9140	6 0 0
11	11	1.9102	1.9096	$\bar{3}$ 3 7
	3		1.8965	3 1 7
3	3	1.8710	1.8688	2 6 4
4	3	1.8399	1.8391	$\bar{6}$ 2 2
10	9	1.8245	1.8256	1 7 3
	3		1.8025	3 5 5
	2		1.7827	5 1 5
11	11	1.7688	1.7683	3 3 7
	2		1.7593	1 1 9
	3		1.7381	3 7 1
9	7	1.7302	1.7304	$\bar{2}$ 4 8
	4		1.7300	0 8 0
15	6	1.6868	1.6885	$\bar{1}$ 7 5
	7		1.6872	$\bar{4}$ 6 4
11	5	1.6760	1.6750	5 3 5
	8		1.6748	6 4 0
4	5	1.6568	1.6555	1 3 9
11	3	1.6504	1.6496	$\bar{6}$ 0 6
5	3	1.6433	1.6238	6 2 4
	3		1.6102	$\bar{5}$ 5 5
6	2	1.6081	1.6053	7 1 1
7	3	1.5943	1.5942	4 0 8

*From crystal structure refinement.
**Calculated from XRPD cell refinement with *a* 11.545 (2), *b* 13.840(2), *c* 16.504(4) Å, β = 95.87(2)°, V = 2623.1 (6) Å^3

Refinement in the acentric space group *C*2 (No. 5), did not greatly improve the *R* value, *R* = 0.042 and 0.032 (all data and observed data), but the systematic absences were gone and there were significant, but small, differences in the occupancy of certain cation sites. This is discussed under the structure description. During the refinement process, it became evident that the *Na*4 and *Si*5 sites were best refined as split sites. In the last stage of refinement, the electron residuals were +1.6 and –0.58 e$^-$/Å^3. In the final least-squares refinement, all atom positions were refined with anisotropic displacement-factors. The weighting

TABLE 3. BUSSYITE-(Y): DATA COLLECTION AND STRUCTURE REFINEMENT INFORMATION

Space Group	*C* 2 (# 5)	Measured reflections	51959
a (Å)	11.600(3)	Unique reflections	7762
b (Å)	13.856(3)	Observed reflections [> 4σ (*F*)]	6531
c (Å)	16.516(4)	*R*(int) (%)	1.97
β (°)	95.84(1)	Goodness of fit on F^2	1.06
V (Å^3)	2641(2)	*R* index (%) for all data	4.24
μ (mm^{-1})	4.93	*R* index (%) for observed data	3.25

Ideal unit-cell contents: $4\{(Y,REE,Ca)_3(Na,Ca)_6Mn[Si_8Be_6(O,OH,F)_{34}]\}$

scheme is inversely proportional to $\sigma^2(F)$. The final positional and anisotropic displacement-parameters are given in Table 4 and selected bond-lengths and angles in Table 5. Tables listing the observed and calculated structure-factors may be obtained from the Depository of Unpublished Data, on the MAC website [document: bussyite-(Y) 53-2_10.3749/canmin.1500005].

Description of the Structure

In the structure of bussyite-(Y) there are four sites containing rare earth elements (*REE*), all with eight-fold coordination. The four sites are split into two pairs, each pair having a pseudo-center of symmetry that correlates with each of the two sites in centric bussyite-(Ce). There is partitioning in these two pairs of sites: one pair (*RE*1- and *RE*11-sites) have a larger scattering factor, a smaller average bond-length, and a higher bond-valence, whereas the second pair (*Ca*1- and *Ca*11-sites) have a smaller scattering factor, a larger average bond-length, and a lower bond-valence. To satisfy these conditions, site assignments were as follows (Table 6). The *RE* sites primarily contain the smaller, heavy rare earth elements (*HREE*) plus Th; $(Y_{0.874}Nd_{0.221}Dy_{0.154}Gd_{0.142}Sm_{0.108}Er_{0.063}Pr_{0.043}La_{0.038}Yb_{0.030}Ho_{0.027}Tb_{0.022}Tm_{0.011}Eu_{0.010}Th_{0.105}Nb_{0.020})_{\Sigma 1.868}$. This gives 99.3 e^- compared with the structure refined site occupancy of 100.3 e^-. The *Ca* sites contain the larger, light rare earth elements (*LREE*); $(Ca_{0.789}Ce_{0.211})_{\Sigma 1}$. This gives 28.0 e^- compared with the refined site-occupancy of 29.4 e^-.

The *Na* sites are quite varied in polyhedral types. The *Na*1, *Na*11, *Na*22, and *Na*3 atoms are bonded to 6 O and 2 F atoms with average bond lengths of approximately 2.53 Å. These eight-coordinated polyhedra are triangular dodecahedra. The *Na*2 and *Na*33 sites are seven-coordinated with 6 O's and 1 F and a somewhat shorter average bond length of 2.50 Å. The polyhedron may be described as a pentagonal bipyramid. The *Na*4 site is split into two equal parts. Each part of the site is bonded to 5 O and 2 F atoms. This *Na* site has the shortest average bond length: 2.48 Å. The eight *Na* sites (one split site, *Na*4) ideally hold six cations. If the occupancy of the sites are refined, all are fully occupied: this gives 66.0 e^- compared with the chemical analysis total of 47.1 e^-. This poor agreement between crystal-structure analysis and electron microprobe analysis may be due to Na loss under the electron beam.

The six-fold co-ordinated site contains the remaining the Mn and Fe: $(Mn_{0.538}Fe_{0.072})_{\Sigma 0.610}$: this gives 15.3 e^- compared with the structure refined occupancy of 13.5 e^-. Perhaps some of these atoms are at the Na sites to make up for the lacking e^-.

There are six regular [SiO_4] tetrahedra at the *Si* 1, *Si* 11, *Si* 3, *Si* 33, *Si* 4, and *Si* 44 sites and six regular [BeO_3F] tetrahedra at the *Be*2, *Be*22 *Be*6, *Be*66, *Be*7, and *Be*77 sites with only very minor Si substitution. The *Si* 5-site is split (Fig. 2) as it is in bussyite-(Ce). The total sof for the site is too large for Si. In addition, the bond lengths (Table 5) for both *Si* 5 sites are long for normal Si–O bonds. One explanation for this would be substitution of Fe and/or Mn at this site, as this would increase the bond lengths. This would also have the effect of lowering the number of electrons at the M3 site, which would agree with the measured value. The pseudo-symmetry related *Si* 55 site is quite different, with Be being slightly dominant, and there is no splitting; this difference is a good confirmation of the lack of a center of symmetry in the structure.

Bussyite-(Y) has a layered structure (Fig. 3) consisting of two slabs of polyhedra; (1) a large slab of Ce-Na-Mn-O polyhedra, and (2) a sheet of Si-Be-tetrahedra. Slabs are cross-linked through shared O atoms but only weakly, as indicated by the perfect $(\bar{1}01)$ cleavage. The slab of high-coordination polyhedra consists of the larger cations Ce, Na, Ca, and Mn. The polyhedra of this layer (Fig. 4) are in two chains: higher bond-valence cations Ce, Ca, and Mn form one polyhedral chain that is cross-linked to the chain of Na polyhedra. There are a number of holes in the sheet that contain the H atoms. The split *Na*4 site also occupies one of these holes one-half of the time *i.e.,* a 0.5 occupancy for each site. The tetrahedral layer (Fig. 5) is made up of a series of cross-linked rings. This is best seen in the net-topology diagram (Fig. 6) where each tetrahedron is represented by a single point. In

TABLE 4. BUSSYITE-(Y): ATOM COORDINATES, ANISOTROPIC-DISPLACEMENT FACTORS (Å^2), AND BOND-VALENCE SUMS (vu)

Site	*x*	*y*	*z*	sof*	U_{11}	U_{22}	U_{33}	U_{23}	U_{13}	U_{12}	U_{eq}	BVS
*Y*1	0.849144(3)	0.255	0.350355(2)	0.8641(1)	0.01577(2)	0.01410(2)	0.01569(2)	–0.00002(1)	–0.00068(1)	–0.00093(1)	0.01534(1)	3.24
*Y*11	0.650974(4)	0.243964(3)	0.149616(2)	0.8655(1)	0.01697(2)	0.01451(2)	0.01415(2)	0.00056(1)	0.00023(1)	0.00074(1)	0.01530(1)	3.24
*Ca*1	0	0.457743(8)	½	0.7668(3)	0.01983(5)	0.01077(4)	0.01178(4)	0	–0.00042(4)	0	0.01427(3)	2.43
*Ca*11	½	0.04138(1)	0	0.7425(3)	0.02005(5)	0.03017(6)	0.01443(5)	0	–0.00032(5)	0	0.02169(3)	2.43
*Na*1	0	0.73632(4)	½	1	0.0597(3)	0.0516(3)	0.0365(3)	0	0.0190(2)	0	0.0483(2)	1.20
*Na*11	0	0.26519(3)	0	1	0.0717(3)	0.0196(2)	0.0239(2)	0	0.0222(2)	0	0.0372(1)	1.20
*Na*2	0.82433(3)	–0.02130(3)	0.33690(2)	1	0.0267(1)	0.0498(2)	0.0210(1)	–0.0100(1)	0.0056(1)	0.0093(1)	0.03230(9)	1.19
*Na*22	0.82865(3)	0.54577(3)	0.35094(2)	1	0.0236(1)	0.0439(2)	0.0195(1)	–0.0005(1)	–0.0020(1)	–0.0007(1)	0.02929(9)	1.25
*Na*3	0.17265(2)	0.46012(3)	0.15190(2)	1	0.0124(1)	0.0646(2)	0.0274(1)	0.0348(1)	0.0031(1)	0.0009(1)	0.03470(9)	1.20
*Na*33	0.82842(3)	0.01641(3)	–0.16316(2)	1	0.0369(2)	0.0446(2)	0.0506(2)	0.0345(1)	0.0001(1)	0.0040(2)	0.0443(1)	1.14
*Na*4A	0.69015(9)	0.74324(5)	0.22217(5)	0.537(1)	0.1243(6)	0.0222(3)	0.0677(4)	0.0013(3)	0.0505(4)	–0.0276(3)	0.0686(3)	1.25
*Na*4B	0.80760(7)	0.75337(5)	0.28205(5)	0.544(1)	0.0957(4)	0.0329(3)	0.0766(3)	0.0055(3)	0.0773(2)	–0.0001(3)	0.0637(2)	1.33
*Mn*1	0	–0.07428(3)	0	0.5342(5)	0.0152(1)	0.0523(2)	0.0389(2)	0	0.0007(1)	0	0.0356(1)	1.32
*Mn*11	½	0.57856(2)	½	0.5183(5)	0.0278(2)	0.0190(1)	0.0250(1)	0	–0.0061(1)	0	0.02453(8)	1.37
Si 1	0.79553(2)	0.097517(1)	0.01596(1)	0.8998(5)	0.01324(7)	0.01159(7)	0.01376(7)	0.00446(6)	0.00444(6)	0.00708(6)	0.01265(4)	4.24
Si 11	0.70946(2)	0.39894(1)	0.48422(1)	0.9701(5)	0.01781(8)	0.01211(7)	0.01232(7)	–0.00479(6)	–0.00396(6)	–0.00251(6)	0.01446(4)	4.24
*Be*2	0.45436(7)	0.09465(8)	0.17246(6)	0.9732(8)	0.0169(3)	0.0427(5)	0.0345(4)	0.0107(4)	0.0156(3)	–0.0112(3)	0.0305(2)	3.69
Si 2	0.45436(7)	0.09465(8)	0.17246(6)	0.027(1)	0.0169(3)	0.0427(5)	0.0345(4)	0.0107(4)	0.0156(3)	–0.0112(3)	0.0305(2)	3.69
*Be*22	0.04981(6)	0.40163(4)	0.32400(4)	0.845(1)	0.0369(3)	0.0105(2)	0.0188(2)	–0.0047(2)	–0.0103(2)	0.0027(2)	0.0229(1)	2.09
Si 22	0.04981(6)	0.40163(4)	0.32400(4)	0.156(1)	0.0369(3)	0.0105(2)	0.0188(2)	–0.0047(2)	–0.0103(2)	0.0027(2)	0.0229(1)	2.09
Si 3	0.91880(2)	0.38854(1)	0.16896(1)	1	0.01637(8)	0.01465(8)	0.01632(7)	–0.00045(6)	–0.00245(7)	–0.00194(6)	0.01606(4)	4.34
Si 33	0.58282(2)	0.10985(1)	0.33059(1)	0.8942(5)	0.01762(8)	0.01273(8)	0.00862(7)	0.00345(6)	–0.00327(7)	–0.00657(7)	0.01331(4)	4.17
Si 4	0.83836(2)	0.25334(1)	0.57452(1)	1	0.01652(7)	0.00973(7)	0.01577(7)	–0.00064(6)	–0.00220(6)	–0.00185(6)	0.01427(4)	4.13
Si 44	0.66063(2)	0.24651(1)	–0.07499(1)	0.9499(6)	0.01381(7)	0.01597(8)	0.01094(7)	–0.00170(6)	–0.00088(6)	0.00214(6)	0.01372(4)	4.24
Si 5A	0.55449(3)	0.31015(2)	0.33705(2)	0.6572(1)	0.02059(8)	0.02086(8)	0.01932(7)	0.00067(7)	–0.00070(7)	0.0021(1)	0.02044(5)	3.56
Si 5B	0.59089(2)	0.38674(2)	0.32319(2)	0.7819(6)	0.0206(1)	0.02086(8)	0.01932(8)	0.00067(7)	–0.00070(7)	0.00206(7)	0.02044(5)	4.00
Si 55	0.90792(2)	0.11169(2)	0.17660(2)	0.4392(5)	0.0085(1)	0.0026(1)	0.0059(1)	–0.00259(9)	0.00070(9)	–0.00050(9)	0.00570(6)	2.35
*Be*55	0.90792(2)	0.11169(2)	0.17660(2)	0.5608	0.0085(1)	0.0026(1)	0.0059(1)	–0.00259(9)	0.00070(9)	–0.00050(9)	0.00570(6)	2.35
Be 6	0.25686(6)	–0.10306(5)	0.03084(4)	0.9451(7)	0.0171(3)	0.0103(2)	0.0098(2)	0.0006(2)	–0.0006(2)	–0.0045(2)	0.0126(2)	2.21
Si 6	0.25686(6)	–0.10306(5)	0.03084(4)	0.0549(7)	0.0171(3)	0.0103(2)	0.0098(2)	0.0006(2)	–0.0006(2)	–0.0045(2)	0.0126(2)	2.21
Be 66	0.75742(6)	0.10546(6)	0.46449(5)	0.9644(7)	0.0085(3)	0.0197(3)	0.0217(3)	0.0061(3)	0.0083(2)	–0.0016(2)	0.0162(2)	2.24
Si 66	0.75742(6)	0.10546(6)	0.46449(5)	0.0356(7)	0.0085(3)	0.0197(3)	0.0217(3)	0.0061(3)	0.0083(2)	–0.0016(2)	0.0162(2)	2.24
*Be*7	0.07869(4)	0.10361(3)	0.31002(3)	0.7938(7)	0.0148(2)	0.0081(2)	0.0144(2)	–0.0031(2)	0.0010(2)	–0.0080(2)	0.0125(1)	3.12
Si 7	0.07869(4)	0.10361(3)	0.31002(3)	0.2062(7)	0.0148(2)	0.0081(2)	0.0144(2)	–0.0031(2)	0.0010(2)	–0.0080(2)	0.0125(1)	3.12
Si 77	0.42310(3)	0.39163(2)	0.18775(2)	0.5475(6)	0.0262(2)	0.0245(2)	0.0226(1)	0.00010(1)	0.0003(1)	0.00910(1)	0.02458(8)	3.37
*Be*77	0.42310(3)	0.39163(2)	0.18775(2)	0.4525(6)	0.0262(2)	0.0245(2)	0.0226(1)	0.00010(1)	0.0003(1)	0.00910(1)	0.02458(8)	3.37
*O*1	0.81715(4)	–0.00554(3)	–0.02244(3)	1	0.0168(2)	0.0095(2)	0.0192(2)	–0.0038(2)	–0.0005(2)	–0.0039(2)	0.0153(1)	2.13

TABLE 4. (CONTINUED)

Site	*x*	*y*	*z*	sof*	U_{11}	U_{22}	U_{33}	U_{23}	U_{13}	U_{12}	U_{eq}	BVS
*O*2	0.90810(4)	0.13122(4)	0.07689(3)	1	0.0213(2)	0.0297(2)	0.0149(2)	0.0016(2)	0.0035(2)	–0.0035(2)	0.0219(1)	1.68
*O*3	0.77823(4)	0.17756(3)	–0.05937(3)	1	0.0229(2)	0.0146(2)	0.0207(2)	0.0065(2)	0.0007(2)	0.0070(2)	0.0195(1)	2.03
*O*4	0.68151(4)	0.10677(4)	0.06905(3)	1	0.0256(2)	0.0205(2)	0.0159(2)	–0.0014(2)	0.0058(2)	0.0008(2)	0.0204(1)	1.84
*O*5	0.82023(4)	0.39555(3)	0.43669(3)	1	0.0138(2)	0.0128(2)	0.0200(2)	–0.0026(2)	0.0002(2)	0.0020(2)	0.01560(1)	1.88
*O*6	0.67870(4)	0.50143(3)	0.52094(3)	1	0.0286(2)	0.0090(2)	0.0300(2)	–0.0016(2)	0.0079(2)	0.0037(2)	0.0222(1)	1.88
*O*7	0.59217(4)	0.36542(4)	0.42418(3)	1	0.0259(2)	0.0196(2)	0.0161(2)	–0.0101(2)	–0.0091(2)	0.0006(2)	0.0213(1)	1.78
*O*8	0.72248(4)	0.32158(4)	0.56125(3)	1	0.0193(2)	0.0277(2)	0.0194(2)	–0.0002(2)	0.0009(2)	0.0063(2)	0.0222(1)	2.11
*O*9	0.82486(4)	0.18915(4)	0.21403(3)	1	0.0172(2)	0.0228(2)	0.0278(2)	–0.0067(2)	–0.0006(2)	0.0058(2)	0.0228(1)	1.51
*O*10	0.86696(4)	0.00002(3)	0.19072(3)	1	0.0216(2)	0.00800(18)	0.0320(2)	–0.0009(2)	–0.0134(2)	0.0021(2)	0.0216(1)	1.34
*O*11	1.04426(4)	0.13167(5)	0.21303(3)	1	0.0151(2)	0.0510(3)	0.0174(2)	0.0030(2)	0.0011(2)	0.0084(2)	0.0278(2)	1.25
*O*12	0.92917(4)	0.37692(4)	0.26881(3)	1	0.0176(2)	0.0292(2)	0.0136(2)	0.0007(2)	–0.0009(2)	–0.0105(2)	0.0203(1)	1.95
*O*13	1.03239(4)	0.50786(3)	0.36529(3)	1	0.0271(2)	0.0048(2)	0.0181(2)	–0.0014(2)	0.0021(2)	–0.0065(2)	0.0167(1)	1.96
*O*14	1.04948(4)	0.32025(3)	0.40203(3)	1	0.0132(2)	0.0153(2)	0.0220(2)	–0.0006(2)	–0.0029(2)	0.0004(2)	0.0171(1)	1.85
*O*15	1.00408(6)	0.30427(4)	0.13757(3)	1	0.0734(4)	0.0263(2)	0.0167(2)	0.0003(2)	–0.0145(3)	0.0248(3)	0.0401(2)	1.42
*O*16	0.46576(4)	–0.01184(4)	0.13747(3)	1	0.0202(2)	0.0269(2)	0.0112(2)	0.0028(2)	–0.0028(2)	–0.0037(2)	0.0197(1)	2.07
*O*17	–0.21267(4)	0.37188(4)	0.13111(3)	1	0.0247(2)	0.0218(2)	0.0117(2)	0.0081(2)	–0.0056(2)	–0.0018(2)	0.0199(1)	2.15
*O*18	–0.28478(4)	0.12677(3)	0.37095(3)	1	0.0104(2)	0.0216(2)	0.0135(2)	–0.0008(2)	–0.0026(2)	–0.0130(2)	0.0154(1)	2.01
*O*19	0.57322(4)	0.12036(3)	0.23302(3)	1	0.0232(2)	0.0136(2)	0.0102(2)	0.0024(2)	–0.0071(2)	–0.0048(2)	0.0163(1)	1.95
*O*20	0.49276(5)	0.18743(4)	0.36426(3)	1	0.0409(3)	0.0260(3)	0.0330(3)	–0.0059(2)	0.0134(2)	0.0152(2)	0.0327(2)	1.64
*O*21	0.84375(3)	0.19108(3)	0.49129(2)	1	0.0108(2)	0.0099(2)	0.0107(2)	–0.0082(1)	–0.0016(1)	–0.0032(2)	0.0106(1)	1.92
*O*22	0.82152(4)	0.17942(3)	0.65101(3)	1	0.0117(2)	0.0170(2)	0.0295(2)	0.0020(2)	–0.0030(2)	0.0085(2)	0.0197(1)	1.83
*O*23	0.45368(4)	0.17576(3)	0.09824(3)	1	0.0213(2)	0.0189(2)	0.0146(2)	0.0101(2)	–0.0002(2)	0.0060(2)	0.0184(1)	1.92
*O*24	0.65189(4)	0.30465(3)	0.00863(3)	1	0.0304(2)	0.0138(2)	0.0174(2)	0.0036(2)	0.0011(2)	0.0035(2)	0.0206(1)	1.93
*O*25	0.67716(4)	0.31959(4)	–0.14945(3)	1	0.0311(2)	0.0243(2)	0.0084(2)	0.0050(2)	0.0070(2)	–0.0057(2)	0.0209(1)	1.84
*O*26	0.45547(4)	0.36819(3)	0.28389(3)	1	0.0240(2)	0.01373(19)	0.0171(2)	–0.0031(2)	–0.0031(2)	0.0010(2)	0.0186(1)	1.50
*O*27	0.67255(4)	0.30943(3)	0.28425(2)	1	0.0209(2)	0.0202(2)	0.0057(2)	–0.0022(2)	–0.0032(2)	0.0081(2)	0.0159(1)	1.59
*O*28	0.96801(4)	0.11570(4)	0.35787(3)	1	0.0130(2)	0.0215(2)	0.0214(2)	–0.0038(2)	0.0049(2)	–0.0036(2)	0.0184(1)	1.04
*O*29	1.13509(5)	0.00272(5)	0.31118(4)	1	0.0351(3)	0.0366(3)	0.0473(3)	0.0066(3)	0.0250(2)	0.0028(3)	0.0383(2)	1.13
*O*30	0.53130(4)	0.38391(3)	0.14053(3)	1	0.0132(2)	0.0193(2)	0.0126(2)	0.0022(2)	0.0012(2)	0.0052(2)	0.01503(1)	1.29
*F*1	0.15875(3)	0.39600(3)	0.28044(2)	1	0.0214(2)	0.0216(2)	0.0102(2)	0.0032(2)	0.0035(1)	0.0009(2)	0.0176(1)	1.10
*F*2	0.34053(4)	0.10113(4)	0.22014(3)	1	0.0259(2)	0.0468(3)	0.0461(3)	0.0055(2)	0.0061(2)	–0.0025(2)	0.0394(2)	0.84
*F*3	0.64117(4)	–0.10185(3)	0.01420(3)	1	0.0215(2)	0.0226(2)	0.0292(2)	0.0038(2)	0.0048(2)	–0.0009(2)	0.0243(1)	0.97
*F*4	0.86423(4)	0.60011(4)	0.48569(3)	1	0.0318(2)	0.0415(3)	0.0164(2)	–0.0012(2)	0.0005(2)	–0.0063(2)	0.0300(1)	0.78

*Site-occupancy factor (sof). Scattering curve is that used in atom name, except for *RE*1 and *RE*11, which use the Ce scattering curve, and *Ca*1 and *Ca*11, which use the Y scattering curve.
**OH by difference with F and Cl total to 4 anions
***Bond-valence sum using constants of Brese & O'Keeffe (1991)

TABLE 5. BUSSYITE-(Y): SELECTED BOND LENGTHS (Å)

*Y*1–O27	2.3456(7)	*Y*11–*O*9	2.3109(7)	*Ca*1–*O*5 × 2	2.3960(7)	*Na*1–*O*20 × 2	2.3352(8)
*Y*1–O28	2.3680(6)	*Y*11–*O*4	2.3677(6)	*Ca*1–*O*13 × 2	2.3965(7)	*Na*1–*F*4 × 2	2.4541(8)
*Y*1–O12	2.4051(6)	*Y*11–*O*30	2.3807(6)	*Ca*1–*F*4 × 2	2.5204(7)	*Na*1–*O*7 × 2	2.4868(8)
*Y*1–O18	2.4070(6)	*Y*11–*O*27	2.3910(7)	*Ca*1–*O*14 × 2	2.6012(7)	*Na*1–*O*8 × 2	2.9237(8)
*Y*1–O9	2.4192(7)	*Y*11–*O*17	2.4157(6)	<*Ca*1–*O F*>	<2.5129>	<*Na*1–*O F*>	<2.5500>
*Y*1–O5	2.4568(6)	*Y*11–*O*19	2.4285(6)	*Ca*11–*O*16 × 2	2.4577(7)	*Na*11–*O*15 × 2	2.3315(8)
*Y*1–O21	2.5972(7)	*Y*11–*O*24	2.4767(7)	*Ca*11–*O*4 × 2	2.4629(7)	*Na*11–*F*3 × 2	2.4604(7)
*Y*1–O14	2.5579(7)	*Y*11–*O*23	2.5408(7)	*Ca*11–*O*23 × 2	2.5624(6)	*Na*11–*O*2 × 2	2.5437(7)
<*Y*1–O>	<2.4446>	<*Y*11–*O*>	<2.4140>	*Ca*11–*F*3 × 2	2.5686(6)	*Na*11–*O*3 × 2	2.9224(8)
				<*Ca*11–*O F*>	<2.5653>	<*Na*11–*O F*>	<2.5653>
*Na*2–*F*1	2.3468(8)	*Na*22–*F*2	2.3097(8)	*Na*3–*F*1	2.3221(7)	*Na*33–*O*1	2.3607(8)
*Na*2–*O*6	2.3727(8)	*Na*22–*F*4	2.3459(7)	*Na*3–*O*10	2.3458(8)	*Na*33–*O*11	2.3787(8)
*Na*2–*O*26	2.3868(7)	*Na*22–*O*29	2.3512(9)	*Na*3–*O*16	2.4190(8)	*Na*33–*F*2	2.3936(8)
*Na*2–*O*18	2.5045(7)	*Na*22–*O*13	2.4091(8)	*Na*3–*F*3	2.4236(7)	*Na*33–*O*30	2.4566(7)
*Na*2–*O*28	2.5266(7)	*Na*22–*O*5	2.5250(7)	*Na*3–*O*4	2.4577(7)	*Na*33–*O*17	2.4976(7)
*Na*2–*O*10	2.5306(8)	*Na*22–*O*22	2.5404(7)	*Na*3–*O*25	2.6159(8)	*Na*33–*O*29	2.5303(8)
*Na*2–*O*8	2.8373(8)	*Na*22–*O*20	2.7277(8)	*Na*3–*O*19	2.8931(7)	*Na*33–*O*3	2.9097(8)
<*Na*2–*O F*>	<2.5008.>	*Na*22–*O*12	2.9992(8)	*Na*3–*O*15	2.9067(9)	<*Na*33–*O F*>	<2.5039>
		<*Na*22–*O F*>	<2.5260>	<*Na*3–*O F*>	<2.5480>		
*Na*4A–*Na*4B	1.606(1)	*Na*4B–*Na*4A	1.606(1)	*Mn*1–*O*1 × 2	2.3202(7)	*Mn*11–*O*6 × 2	2.3265(7)
*Na*4A–*O*11	2.286(1)	*Na*4B–*O*22	2.203(1)	*Mn*1–*O*30 × 2	2.3839(7)	*Mn*11–*O*21 × 2	2.3840(7)
*Na*4A–*O*22	2.290(1)	*Na*4B–*O*26	2.337(1)	*Mn*1–*O*24 × 2	2.4265(7)	*Mn*11–*O*28 × 2	2.4265(7)
*Na*4A–*O*25	2.304(1)	*Na*4B–*F*2	2.392(1)	<*Mn*1–*O*>	<2.3769>	<*Mn*11–*O*>	<2.3790>
*Na*4A–*F*1	2.369(1)	*Na*4B–*O*25	2.398(1)				
*Na*4A–*O*15	2.591(1)	*Na*4B–*O*20	2.588(1)				
*Na*4A–*F*2	2.633(1)	*Na*4B–*F*1	2.623(1)				
*Na*4A–*O*3	2.897(1)	*Na*4B–*O*8	2.810(1)				
<*Na*4A–*O F*>	<2.4814>	<*Na*4B–*O F*>	<2.4787>				

TABLE 5. (CONTINUED)

*Si*1–*O*1	1.5928(6)	*Si*11–*O*5	1.5731(6)	*Be*2–*O*16	1.595(1)	*Be*22–*F*1	1.518(1)
*Si*1–*O*2	1.6337(6)	*Si*11–*O*6	1.5988(6)	*Be*2–*F*2	1.607(1)	*Be*22–*O*12	1.627(1)
*Si*1–*O*3	1.6635(6)	*Si*11–*O*8	1.6587(6)	*Be*2–*O*19	1.658(1)	*Be*22–*O*13	1.643(1)
*Si*1–*O*4	1.6646(6)	*Si*11–*O*7	1.6660(6)	*Be*2–*O*23	1.663(1)	*Be*22–*O*14	1.713(1)
<*Si*1–*O*>	<1.6387>	<*Si*11–*O*>	<1.6242>	<*Be*2–*O F*>	<1.631>	<*Be*22–*O F*>	<1.626>
*Si*3–*O*16	1.5907(6)	*Si*33–*O*19	1.6105(6)	*Si*4–*O*14	1.6123(6)	*Si*44–*O*24	1.6109(6)
*Si*3–*O*17	1.6049(6)	*Si*33–*O*18	1.6278(6)	*Si*4–*O*21	1.6295(5)	*Si*44–*O*25	1.6194(6)
*Si*3–*O*15	1.6478(7)	*Si*33–*O*20	1.6354(7)	*Si*4–*O*8	1.6398(6)	*Si*44–*O*23	1.6622(6)
*Si*3–*O*12	1.6490(6)	*Si*33–*O*13	1.6542(6)	*Si*4–*O*22	1.6535(6)	*Si*44–*O*3	1.6639(6)
<*Si*3–*O*>	<1.6231>	<*Si*11–*O*>	<1.6320>	<*Si*4–*O*>	<1.6338>	<*Si*44–*O*>	<1.6391>
*Si*5A–*Si*5B	1.1733(5)	*Si*5B–*Si*5A	1.1733(5)	*Be*55–*O*9	1.6075(6)	*Be*6–*F*3	1.4602(9)
*Si*5A–*O*26	1.5912(6)	*Si*5B–*O*27	1.6069(6)	*Be*55–*O*10	1.6422(6)	*Be*6–*O*1	1.5933(8)
*Si*5A–*O*7	1.6493(6)	*Si*5B–*O*26	1.6576(7)	*Be*55–*O*11	1.6562(7)	*Be*6–*O*17	1.6937(9)
*Si*5A–*O*27	1.6967(7)	*Si*5B–*O*7	1.6925(7)	*Be*55–*O*2	1.6691(7)	*Be*6–*O*24	1.7781(9)
*Si*5A–*O*20	1.9163(7)	*Si*5B–*O*29	1.7046(8)	<*Be*55–*O*>	<1.6438>	<*Be*6–*O F*>	<1.6313>
<*Si*5A–*O*>	<1.7134>	<*Si*5B–*O*>	<1.6654>				
*Be*66–*O*21	1.586(1)	*Be*7–*O*29	1.5428(8)	*Si*77–*O*30	1.5473(7)		
*Be*66–*O*18	1.600(1)	*Be*7–*O*28	1.5836(8)	*Si*77–*O*25	1.6123(7)		
*Be*66–*O*6	1.628(1)	*Be*7–*O*22	1.6449(7)	*Si*77–*O*26	1.6267(6)		
*Be*66–*F*4	1.706(1)	*Be*7–*O*11	1.6573(8)	*Si*77–*O*10	1.6397(7)		
<*Be*66–*O F*>	<1.6300>	<*Be*7–*O*>	<1.6702>	<*Si*77–*O*>	<1.6065>		

TABLE 6. BUSSYITE-(Y): DERIVATION OF EMPIRICAL FORMULA

Site	*apfu* (chemical analysis)	e^- in empa	epfu crystal structure	Valence	BVS
*M*1a	$(Y_{0.874}Nd_{0.221}Dy_{0.154}Gd_{0.142}$ $Sm_{0.108}Er_{0.063}Pr_{0.043}La_{0.038}Yb_{0.030}Ho_{0.027}$ $Tb_{0.022}Tm_{0.011}Eu_{0.010}Th_{0.105}Nb_{0.020})_{\Sigma 1.868}$	99.3	100.3	5.74^+	5.95^+
*M*1b	$(Ca_{0.789}Ce_{0.211})_{\Sigma 1}$	28.0	29.4	2.44+	2.54^+
*M*2	$(Na_{3.449}Ca_{0.430}K_{0.022}Ba_{0.003})_{\Sigma 3.904}$	47.1	66.0	5.34^+	7.26^+
*M*3	$(Mn_{0.538}Fe_{0.072})_{\Sigma 0.610}$	15.3	13.15	1.22^+	0.87^+
*M*4	$(Si_{8.585}Be_{5.075}Al_{0.074})_{\Sigma 13.73}$	141.4	142.9	44.7^+	46.8^+
∑cation				**<58.10$^+$>**	
*X*1	$(O_{24.226}OH_{5.774})_{\Sigma 30}$			54.23^-	
*X*2	$(F_{2.392}OH_{1.597}Cl_{0.011})_{\Sigma 4}$			4^-	
∑anion				**<58.23$^-$>**	

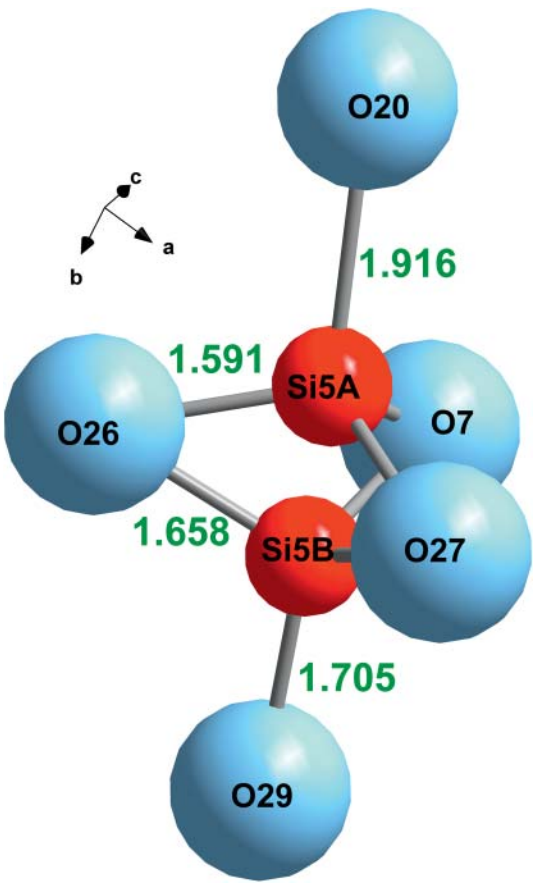

FIG. 2. The *Si*5 site in bussyite-(Y). Distances (Å) between *Si* 5, *Si* 5a, and O sites.

bussyite-(Y), the tetrahedral layer is composed of four-, five- and eight-connected rings. This is the same topology as bussyite-(Ce), but the composition of the layer is somewhat different due to the decrease in Si : Be ratio. Because of the lack of a center of symmetry in bussyite-(Y), the *Si* 5/*Be*55 and *Be*7/*Si* 77 sites are no longer related by a center of symmetry and can have different occupancies, as they do with an increased Be content. All other tetrahedral sites have similar occupancies. Another difference between the two structures is that bussyite-(Y) has only one-half of the eight-connected rings with a split tetrahedral site (*Si* 5A and B) while all eight-connected rings in bussyite-(Ce) contain a split site.

The role of hydrogen in bussyite

The infrared spectrum for bussyite-(Y) differs from that of bussyite-(Ce) (Grice *et al.* 2009) in the regions relevant to the presence of $[OH]^-$ ions and $[H_2O]$ groups. It is evident that H is much more abundant in bussyite-(Ce) as $[H_2O]$ groups at Na-vacant sites. Bussyite-(Ce) has two coexisting phases, a Na-poor phase with $[H_2O]$ groups and a Na-rich phase that is anhydrous. There is minor substitution of OH for F. There are no $[H_2O]$ groups in bussyite-(Y) and OH groups are at O and F sites coordinated to Be. The amount of H in both minerals is approximately equal in weight percent.

Related structures

Bussyite-(Y) and bussyite-(Ce) are topologically similar but differ in structural details. Table 7 compares the two minerals; bussyite-(Y) has a smaller cell volume, higher density, and higher refractive indices. They cannot be systematically differentiated by XRPD but the chemical composition differs in

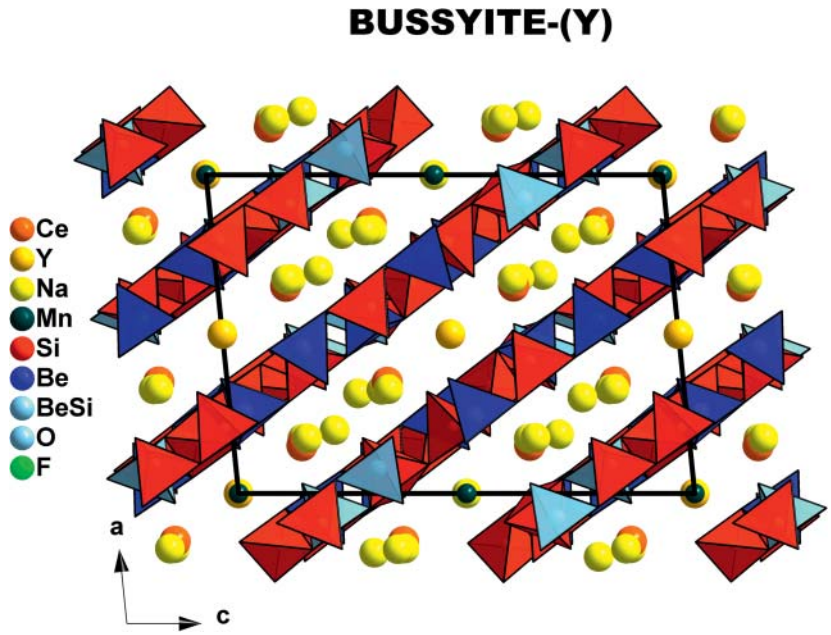

FIG. 3. The layered structure of bussyite-(Y) projected along [010]. The [SiO_4] tetrahedra are red, the [BeO_4] tetrahedra blue, Ce atoms in red, Ca atoms in orange, Na atoms in yellow, and Mn in grey.

REE content and Be/Si content. The most significant structural difference is in the space group, with a transition from centrosymmetric bussyite-(Ce) to non-centrosymmetric bussyite-(Y). This seemingly subtle change primarily manifests itself in the tetrahedral layer through differences in Si and Be site occupancies that were previously symmetry equivalent.

The relationship of bussyite-(Ce) to other minerals, melilite group minerals, aminoffite, semenovite-(Ce), and harstigite, is discussed in detail in Grice *et al*. (2009).

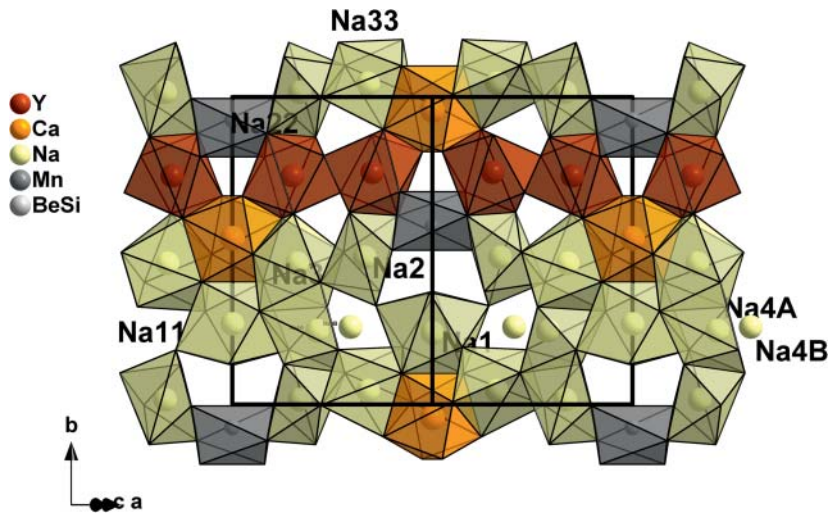

FIG. 4. Large-cation layer in the bussyite-(Ce) structure: [CeO_8] polyhedra are in red, [CaO_8] polyhedra in orange, [NaO_n] polyhedra in yellow, and [MnO_6] octahedra in grey.

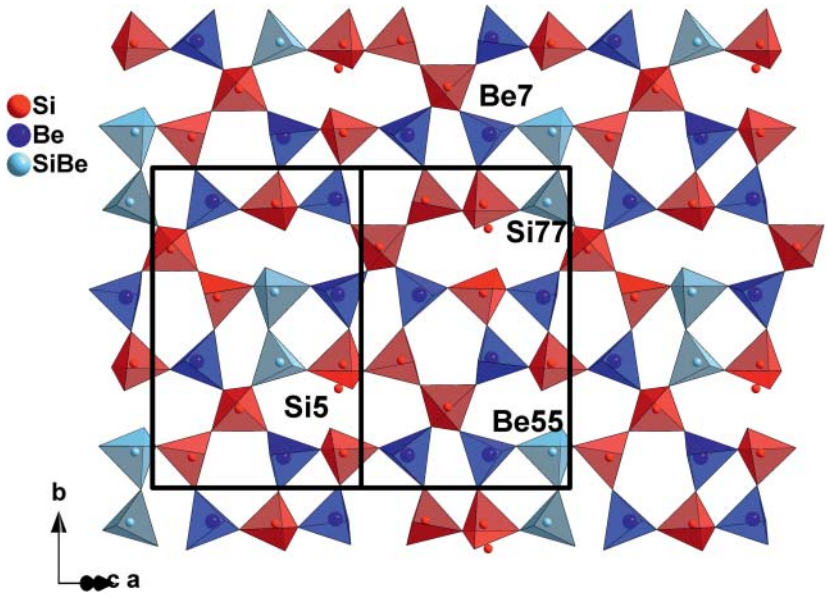

FIG. 5. Tetrahedral layers in the bussyite-(Y) structure: [SiO_4] tetrahedra are red, the [BeO_4] tetrahedra are dark blue, and mixed site [(Si,Be)O_4] are pale blue.

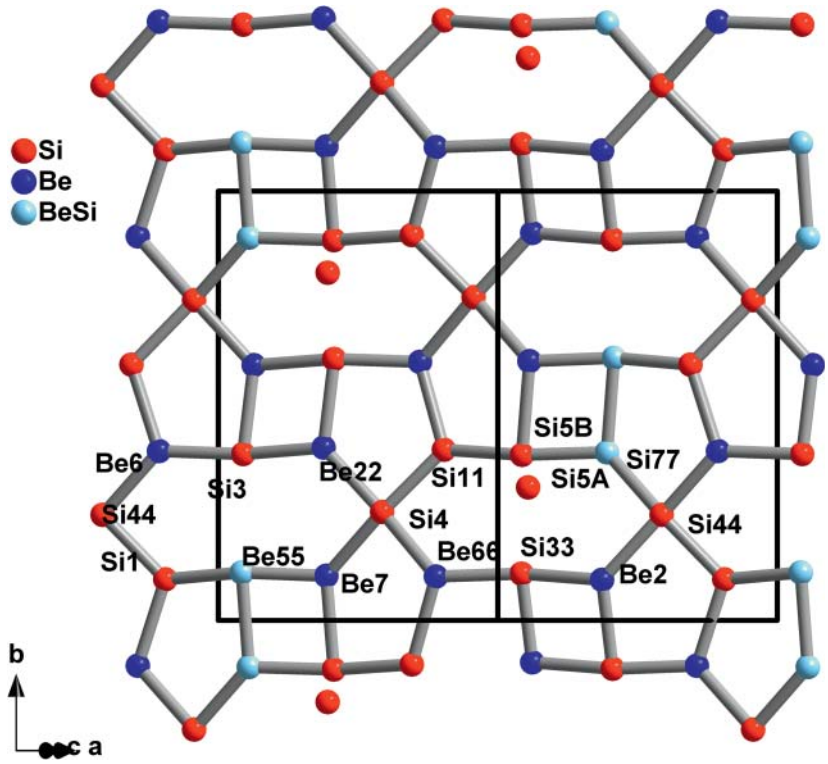

FIG. 6. Topology of the tetrahedral layer in bussyite-(Y). [SiO_4] tetrahedra are represented by red circles, [BeO_4] tetrahedra by dark blue circles, and mixed site [(Si,Be)O_4] by pale blue circles.

TABLE 7. BUSSYITE-(Y) AND BUSSYITE-(Ce) COMPARED

	Bussyite-(Y)	Bussyite-(Ce)
Space Group	*C*2 (# 5)	*C*2*c* (# 15)
a (Å)	11.600(3)	11.654(3)
b (Å)	13.856(3)	13.916(3)
c (Å)	16.516(4)	16.583(4)
β (°)	95.84(1)	95.86(2)
V (Å^3)	2641(2)	2675.4(8)
Formula	(Y,*REE*,Ca)$_3$(Na,Ca)$_6$ $MnSi_8Be_6(O,OH)_{30}(F,OH)_4$	(Ce,*REE*,Ca)$_3$(Na,$H_2O)_6$ $MnSi_9Be_5O_{30}(F,OH)_4$
D calc g/cm^3	3.20	3.11
α	1.583	1.574
β	1.593	1.591
γ	1.600	1.597
2V°(calc)	–68	–63
hkl	*d* (Å), (*I*)	*d* (Å), (*I*)
1$\bar{1}$1	8.049(100)	8.120(100)
020	6.924(21)	6.959(26)
311	3.529(38)	3.543(39)
1$\bar{3}$3	3.435(21)	3.454(21)
1$\bar{5}$5	3.155(23)	3.176(19)
3$\bar{3}$1	2.940(35)	2.959(24)
331	2.840(50)	2.863(48)
006	2.736(30)	2.749(23)
1$\bar{3}$5	2.651(38)	2.668(33)
402	2.629(30)	2.651(0)

Conclusions

Bussyite-(Y) and bussyite-(Ce) are not truly isostructural but are topologically similar. Splitting of the *Si* 5-site is consistent for all three bussyite structures refined [two for bussyite-(Ce) and one for bussyite-(Y)]. Splitting of the *Na*4 position is also consistent for all structural analysis done to date. The role of H differs in the two species; in bussyite-(Ce) H is present in both [H_2O] and [OH] groups, whereas in bussyite-(Y) there are only [OH] groups.

Acknowledgments

The authors gratefully acknowledge the cooperation of, and samples provided by Giles Haineault. The authors thank Dr. Frank Hawthorne, University of Manitoba, for the use of his four-circle diffractometer, Mark Cooper, University of Manitoba for technical assistance, and Elizabeth Moffatt of the Canadian Conservation Institute for the infrared spectrum. Helpful comments were received from Dr. Igor Pekov and Dr. Frank Hawthorne as reviewers, Associate Editor Dr. Henrik Friis and Editor Dr. Lee Groat, improved the quality of the manuscript.

References

Brese, N.E. & O'Keeffe, M. (1991) Bond-valence parameters for solids. *Acta Crystallographica* **B47**, 192–197.

Bussy, A.B. (1828) Préparation du glucinium. *Journal de Chimie Médical, de Pharmacie et de Toxicologie* **4**, 455–456.

Cherniak, D.J., Pyle, J., & Rakovan, J. (2004) Synthesis of *REE* and Y phosphates by Pb-free flux methods and their utilization as standards for electron microprobe analysis and in design of monazite chemical U-Th-Pb dating protocol. *American Mineralogist* **89**, 1533–1539.

Farmer, V.C. (1974) The Infrared Spectra of Minerals. *Mineralogical Society Monograph of Great Britain* **4**, 539 pp.

Grew, E.S. (Ed.). (2002) Beryllium: Mineralogy, Petrology and Geochemistry. *Reviews in Mineralogy* **50**, The Mineralogical Society of America, Washington, United States.

Grice, J.D. (2010) The role of beryllium in beryllosilicate mineral structures and zeolite formation. *Canadian Mineralogist* **48**, 1493–1518.

Grice, J.D., Rowe, R., Poirier, G., Pratt, A., & Francis, J. (2009) Bussyite-(Ce), a new beryllium silicate mineral species from Mont Saint-Hilaire, Quebec. *Canadian Mineralogist* **47**, 193–204.

Pouchou, J.L. & Pichoir, F. (1984) Quantitative microanalytic possibilities using a new formulation of matrix effects. *Journal de Physique* **45**, 17–20 (in French).

Raade, G. (2008) Beryllium in alkaline rocks and syenitic pegmatites. *Norsk Bergverksmeums skriftserie* **37**, Norwegian Mining Museum, Kongsberg, Norway.

Rowe, R. (2009) New statistical calibration approach for Bruker AXS D8 Discover microdiffractometer with Hi-Star detector using GADDS software. *ICDD Powder Diffraction Journal* **24**, 263–271.

Sheldrick, G.M. (1990) *SHELXTL, a crystallographic computing package, revision 4.1*. Siemens Analytical Instruments, Inc., Madison, Wisconsin, United States.

Sheldrick, G.M. (1998) *SADABS User Guide*. University of Göttingen, Göttingen, Germany.

Received January 12, 2015, revised manuscript accepted March 25, 2015.